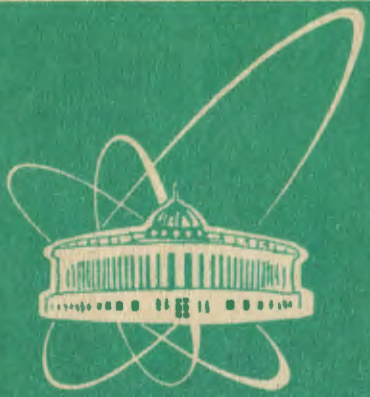

объединенный
институт
ядерных
исследований
дубна

E7-93-278

MULTIFRAGMENTATION IN ^{4}He+Au COLLISIONS AT RELATIVISTIC ENERGIES, STUDIED WITH THE 4π-SETUP FASA

Contribution to the International School-Seminar on Heavy Ion Physics, Dubna, May 10—15, 1993

1993

1 Introduction

The nuclear multifragmentation has been of great experimental and theoretical interest in the last years. There are two reasons for that. First, multifragment emission is the main decay mode of highly excited nucleus. Secondly, the breakup mechanism is not clear yet. A still open question is whether the emission of the intermediate mass fragments (IMF, $3 \leq Z \leq 20$) can be understood by evaporation like process [1], [2], or it is a new phenomenon of hot and diluted nuclear matter, where the emission occurs within very short time. This "simultaneous breakup" mechanism has been associated with volume instabilities [3], [4], which are related to a liquid–gas phase transition in nuclear matter [5], or with surface instabilities which can arise if a system attains some unusual shapes [6], [7].

The experimental studies of multifragment emission have been conducted in the last years by means of 4π–setups on heavy ion beams at both intermediate [8], [9] and high energies [10], [11]. Two questions should be answered by experimentalists in this field: (i) What is the best projectile–target–beam energy combination to prepare the hot nuclear system? (ii) Which are the key observables that give an access to the important physical parameters of the process, like time scale and breakup density?

In this paper we present the first results of our investigations using the extreme case of the very asymmetric system $^4He + {}^{197}Au$ at incident energies up to 3.6 GeV/nucleon. This selection is favoured by various reasons: (i) All detected IMF's are emitted from the target spectator and there is no mixture of different sources like in heavy–ion reactions. (ii) The low center–of–mass velocity allows one to determine with high precision the relative velocities and the relative angular correlations from which the geometry and the time scale of the decay process can be deduced as done in earlier experiments [12], [13]. (iii) Further, with ^4He projectiles dynamical effects are small and the compression of the target nucleus is negligible. Therefore, complementary information to heavy–ion collisions, where these effects are important, is obtained.

In the first part of this paper a short description of a new 4π setup "FASA" is given. Then the data on the fragment mass–spectra will be presented. Further we concentrate on the question whether sufficient excitation energies are reached in our collision system in order to produce a high IMF multiplicity. Then the experimental data on the fragment–fragment correlation at large and small relative angles are discussed to extract information on the breakup density and the time–scale of the process.

2 4π–setup FASA

The experiments were performed at the synchrophasotron of the JINR (Dubna) using the new 4π–device FASA [14].

The general view of FASA is shown in Fig. 1. The main idea of this setup is to

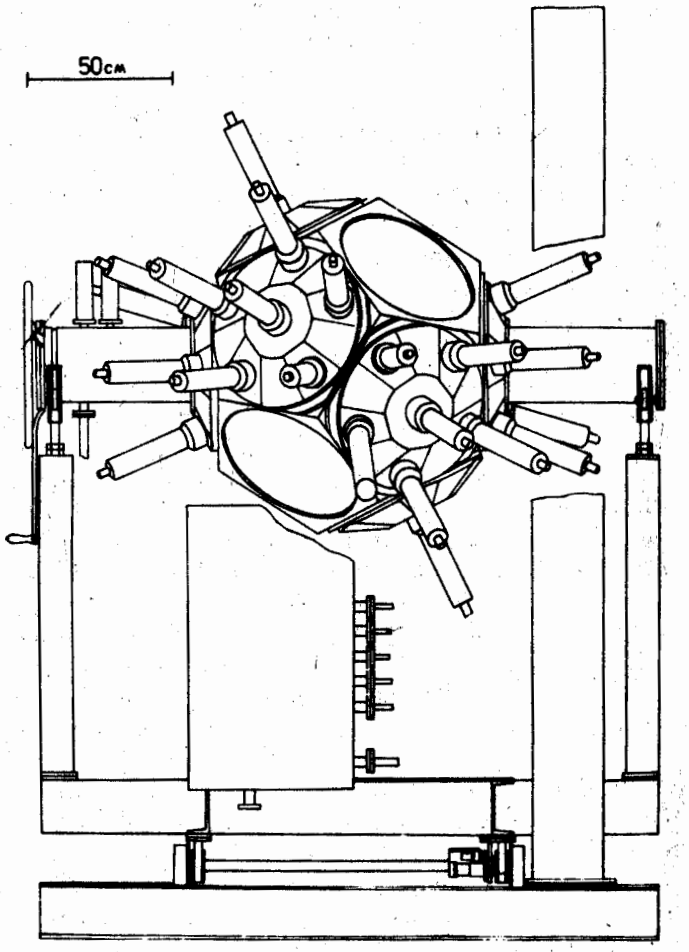

Figure 1: General view of the 4π setup FASA.

determine with high precision the energy, velocity and mass of some fragments of the collision, while for the other fragments only multiplicity information and space distribution are obtained. The main parts of the device are: (i) The fragment multiplicity detector (FMD), consisting of 55 thin (50 μm) CsI(Tl) detectors, which covers the main part of 4π. The scintillators give via their ΔE information the multiplicity of light charged particles (LCP) or of IMF's. (ii) Five time–of–flight telescopes (TOF) which measure the energy, velocity and mass of fragments at selected laboratory angles (117°, 103°, 94°, 68°, 50°), and serve as a trigger for the readout of the system. (iii) A position–sensitive parallel–plate avalanche counter (PPAC), which allows one to determine angular and velocity distributions of fragments detected in coincidence with the time–of–flight telescope. Details of the detectors and their calibration are given in Ref. [14]. Self–supporting ^{197}Au targets 1.0 mg/cm^2 thick and ^4He–beam energies of 1.0 and 3.6 GeV/nucleon at intensities of 5×10^8 particles/spill were used. The beam with a typical half width of 3×1 cm^2 was accompanied by a halo of fast particles, producing background pulses in the CsI(Tl) scintillators and the light guides of the FMD. Using a pulse–shape analysis this background was reduced to the level less than 10% for all scintillators of the FMD, except three ones at the lower incident energy. These three were substracted in the off–line analysis.

3 Mass yield of fragments

By measuring the multiplicity of IMF's and LCP's the 4π setup FASA gives the possibility of examining various observables as a function of the excitation energy reached in the collision system under study. In figure 2 the mass distributions measured in all five TOF (added since they are very similar) are given as a function of the measured LCP multiplicity ($Z \leq 2$), detected in the FMD array and not corrected for efficiency. LCP multiplicity is directly related to the excitation energy of a target spectator [15]. For low LCP multiplicities the mass distributions show two contributions. One is from heavy fragments in the mass region around A = 80, most likely fission fragments. This contribution rapidly disappears with increasing LCP multiplicity, reflecting an increasing excitation energy. The second component represents light masses seen at all the chosen LCP multiplicities. The mass yield in this region is well described by $A^{-\tau}$ dependence for masses between $10 \leq A \leq 40$. The exponent τ is shown at the bottom of figure 2 as a function of the LCP multiplicity, and a minimum is observed at measured multiplicities of 2–4 light charged particles. The minimum in dependence of the τ–parameter on the excitation energy is expected at the critical point for a liquid–gas phase transition [5]. But such a "critical behaviour" may be also simulated by the effect of the secondary decay of the excited fragments, which both enhances the yield of the lighter IMF's and decreases the mean multiplicity of the fragments. This topic needs further investigation. Such a minimum of the τ parameter has also been reported by the ALADIN collaboration [6]. There the τ parameter was deduced as a function of the quantity Z_{bound}. Both observables, M_{LCP}

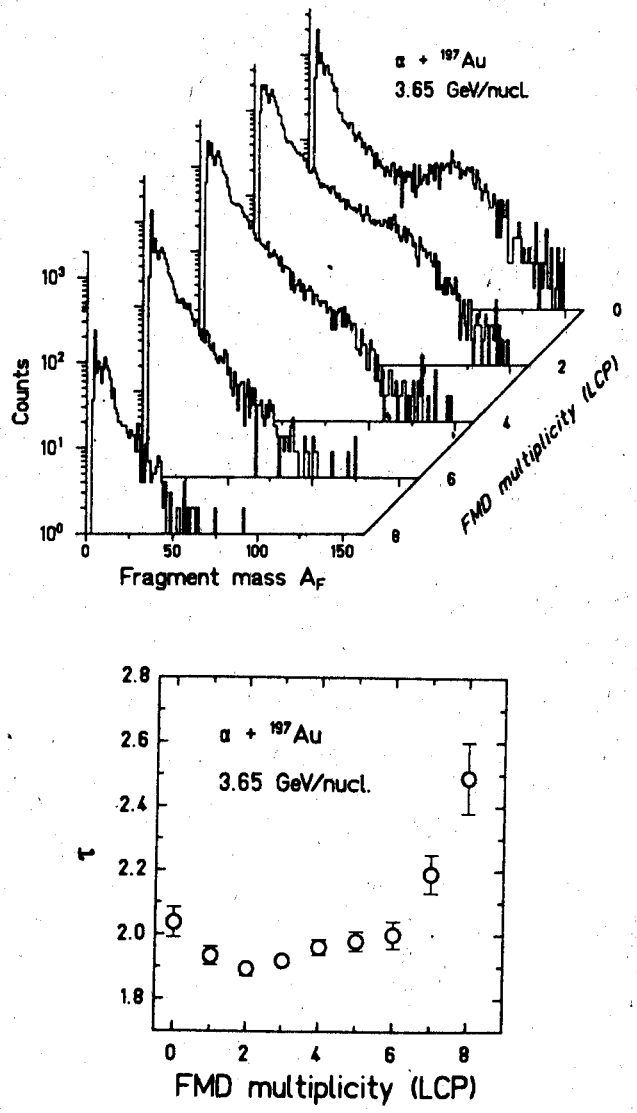

Figure 2: Mass spectra measured in TOF telescopes as a function of the LCP's multiplicity, measured in the fragment multiplicity detector. The bottom part gives the τ–parameter deduced from the mass spectra in the region $10 \leq A \leq 40$.

and Z_{bound}, reflect a measure of the excitation energy. In the ALADIN experiment the minimum in τ is observed at values of Z_{bound} where also the largest mean IMF multiplicity is seen. So the observation of the minimum of the τ parameter in our experiment gives evidence that the region of maximum IMF multiplicity can be also reached with relativistic ^4He–projectiles.

The total cross–section for the fragmentation process for higher incident energy was estimated to be equal to $\sigma_{MF} \simeq 400$ mb. It is significant part of the total inelastic cross–section (15–20%). In fact all the "central" collisions are followed by a multifragment decay of the target spectator. The value of σ_{MF} is related to σ_{IMF} (the production cross–section for IMF) through a simple equation: $\sigma_{MF} = \sigma_{IMF} / < M_{IMF} >$. Our data on the mean intermediate mass fragment multiplicity $< M_{IMF} >$ are presented in the next section.

4 IMF multiplicity and excitation energy

Fig. 3 shows the multiplicity distributions measured by the multiplicity detector. Two distributions are shown: one of them for the events selected by requiring one IMF in a TOF telescope (open circles) and second one for the events selected by fission fragment coincidences in the TOF–telescope and PPAC (open boxes).

To deduce primary multiplicities one has to take into account the fact that the readout is triggered by the TOF telescopes, covering only a small solid angle. Therefore, the trigger probability is proportional to the multiplicity in the event. The experimental distributions are further influenced by the efficiencies of the counters of FMD, the solid angle coverage and the probability of double hits in the counters. All these effects have been combined in a response matrix, representing the experimental filter. The primary distributions were assumed to be Poisson–distributed for higher mean multiplicities and exponential–shaped for the lower ones. Their mean values were deduced by fitting the primary distributions, folded by the experimental filter, to the experimental ones. The result is shown in Fig. 3: folded Poisson distribution describes very well the experimental multiplicity distribution for the process of the multifragment decay, a folded exponential distribution fits well the measured multiplicities of IMF accompanying the fission of the target spectator. The mean values of the primary multiplicities are summarized in table 1 for the two classes of the events at both incident energies.

For the fission events the mean IMF multiplicities are around 1. It means that ternary fission, being a very rare process at low excitation energies, became the main fission mode. The reason for that is evidently very high excitation energy of the fissioning nucleus. Fig. 4 presents the mean IMF multiplicities for the fission class events as a function of the excitation energy. The excitation energies E_x were deduced from the measured fission fragment mass spectra according to the procedure described in ref. [12]. Two values of E_x (from 500 MeV to 700 MeV) for each incident energy correspond to two opening angles between fission fragment detected.

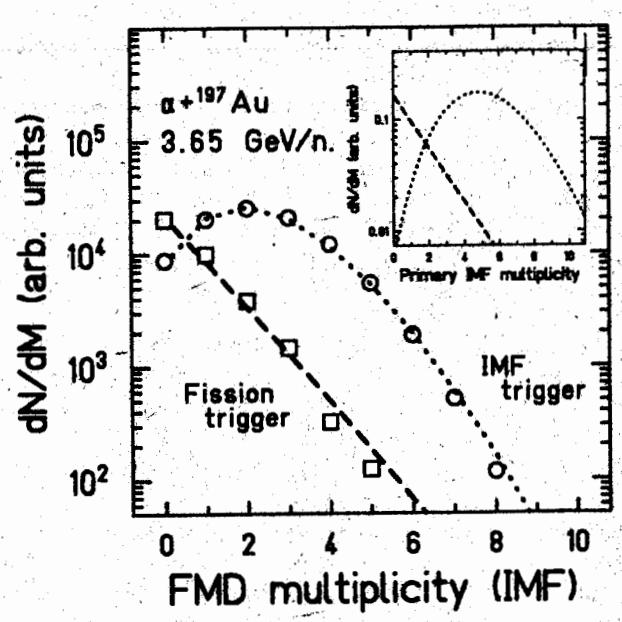

Figure 3: Multiplicity distributions measured in the FMD when selecting fission fragment coincidences (open boxes) and when requiring one IMF in a TOF (open circle). They are fitted with exponential (dashed line) and Poisson (dotted line) distributions, folded with the experimental filter. The insert gives the corresponding primary distributions.

Table 1: The mean primary IMF multiplicities observed in coincidence with the fission or for events with one IMF in one of the TOF telescopes

Event class	1 GeV/nucl.	3.65 GeV/nucl.
Fission	1.1 ± 0.2	1.1 ± 0.2
IMF	3.6 ± 0.6	5.3 ± 0.8

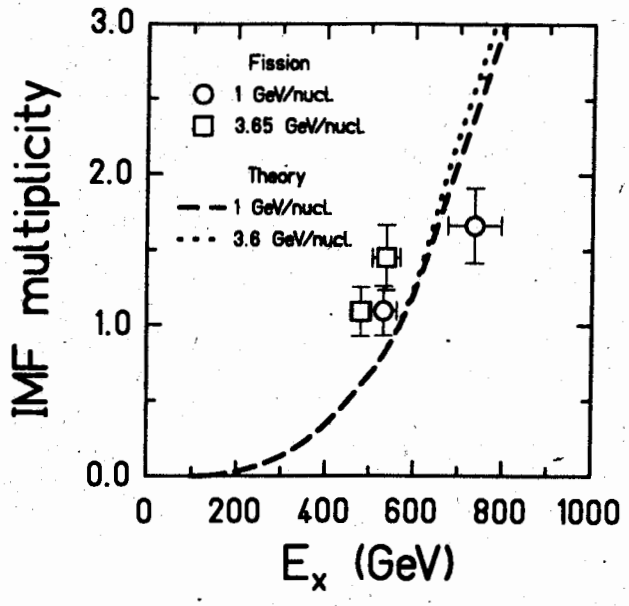

Figure 4: The mean IMF–multiplicities for the fission class events as a function of the excitation energy.

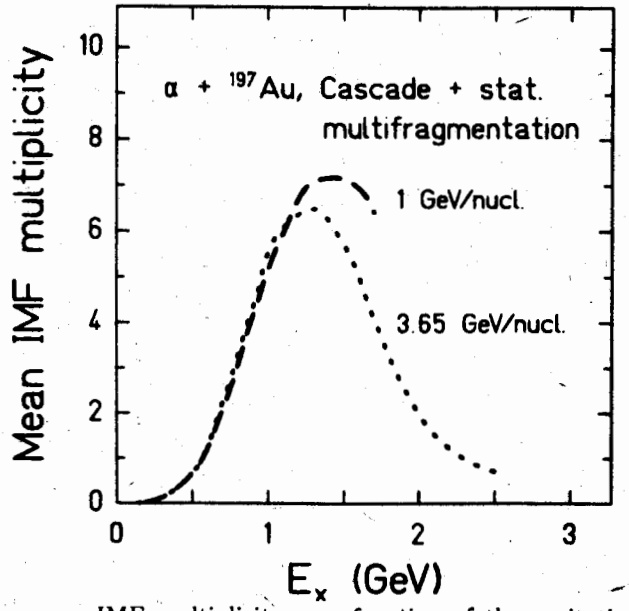

Figure 5: The mean IMF–multiplicity as a function of the excitation energy calculated by the cascade–fragmentation model for 1 GeV/nucl. (dashed line) and 3.65 GeV/nucl. (dotted line) incident energies.

Theoretical curves in Fig. 4 are obtained by the model of ref. [15]. The masses and the excitation energies of the residual nuclei are calculated within an intranuclear–cascade approach. The disassembly of the residual nucleus is then described by a statistical multifragmentation model. In Fig. 5 the mean IMF multiplicities calculated by this model are given as a function of the excitation energy of a target spectator for the $^4He + Au$ interaction. Very fast increase of the multiplicity is predicted with increasing of the excitation energy up to ~ 1.5 GeV. But after that the multiplicity goes down, the behaviour known as "rise and fall of the multifragmentation" [16]. This behaviour is a result of the effect of a secondary decay of the very hot fragments: the overheated system starts to disassembly mainly into light fragment with $A \leq 4$.

For the IMF trigger the mean primary multiplicity is much higher than for the fission trigger and it increases by 50%, when the beam energy is changed from 1 GeV/nucleon to 3.65 GeV/nucleon (see table 1). The calculated IMF–multiplicity distribution looks like a step–function. But it becomes to be a Poisson–like, taking into account the trigger condition of at least one IMF being in a laboratory angle range, covered by the TOF–telescopes. The mean value for IMF multiplicity, calculated by this model, is consistent with the experiment within error bars at higher beam energy.

For higher incident energy the model predicts the excitation energies up to 2.5 GeV with the mean value arouns 1.3 GeV.

5 Breakup density and time scale

The density of the nuclear system at the moment of the beakup is a question of great interest when studying multifragmentation. Due to the Coulomb repulsion the relative velocities of IMF's detected at large relative angles are determined by the geometry of the nuclear system at the instant of their emission. Studying the system $^4He + {}^{197}Au$ at 800 MeV/nucleon incident energy the relative velocities deduced for IMF coincidences with large relative angles were consistent with simultaneous breakup of a dilute system and in contradiction to sequential emission from a residual nucleus with usual nuclear density [17]. In ref. [18] it was argued that the IMF's might be emitted at a very late stage of the de–excitation process, as predicted by a sequential model. Then, the lighter recoiling nucleus reduces the relative velocities leading to a possible description of the measured relative velocity distribution with sequential emission as well. Taking into account the large multiplicities observed in the present experiments, the picture of late and sequential emission of the IMF seems very unlikely, thus supporting disagreement with the sequential scenario, pointed out in Ref.[17].

In the present experiment the relative velocities of IMF at large correlation angles ($\theta_{rel} = 130° \div 180°$) measured at 1 GeV/nucleon incident energy are in agreement with the findings at 800 MeV/nuclon. Going to the 3.65 GeV/nucleon incident energy the mean value of the relative velocity decreases by 0.2 cm/ns, as demonstrated in

Fig. 6. This reduction of the Coulomb repulsion is either due to a larger breakup volume or to a lighter breakup system or to both effects.

Upper part of Fig. 7 shows the mean values for the relative velocities of coincident fragments, measured at large correlation angles, in a function of a mean associated IMF multiplicity $< M >_{aso}$. The last one is obtained from the multiplicity measured by FMD, taking into account its eficiency and multiplicity distribution for IMF–IMF trigger at the respective beam energy.

Lower part of Fig. 7 presents the mean relative velocity at the same correlation angles, calculated by the cascade–statistical multifragmentation model. One of the parameters of this model is a breakup density ρ_f. The results in Fig. 7 were obtained for $\rho_f/\rho_o = 1/3$. The calculated values of the mean relative velocities are significantly larger than the experimental one for small multiplicities and slightly above for higher $< M >_{aso}$. So one can conclude from this comparison, that the freeze–out density ρ_f is less than $1/3\rho_o$.

The experimental values of $< V_{rel} >$ are slightly decreasing with the increase of

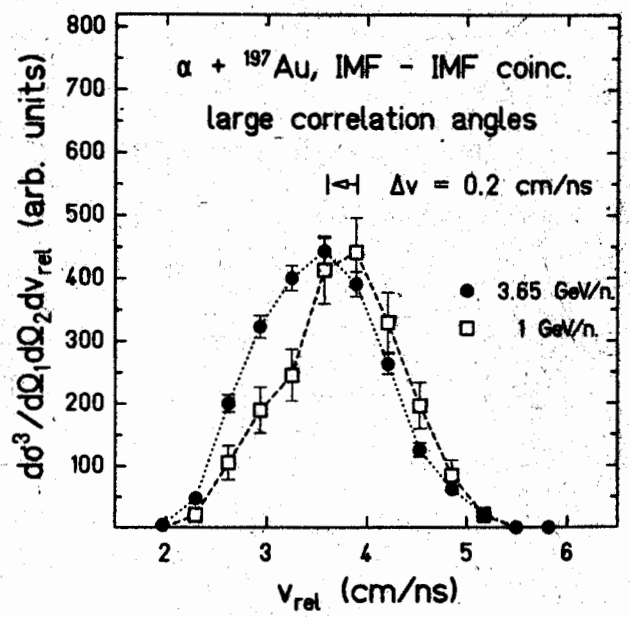

Figure 6: Relative velocities of IMF–IMF coicidences for the large correlation angles at 1 GeV/nucl. (open boxes) and 3.65 GeV/nucl. (open circles) incident energy.

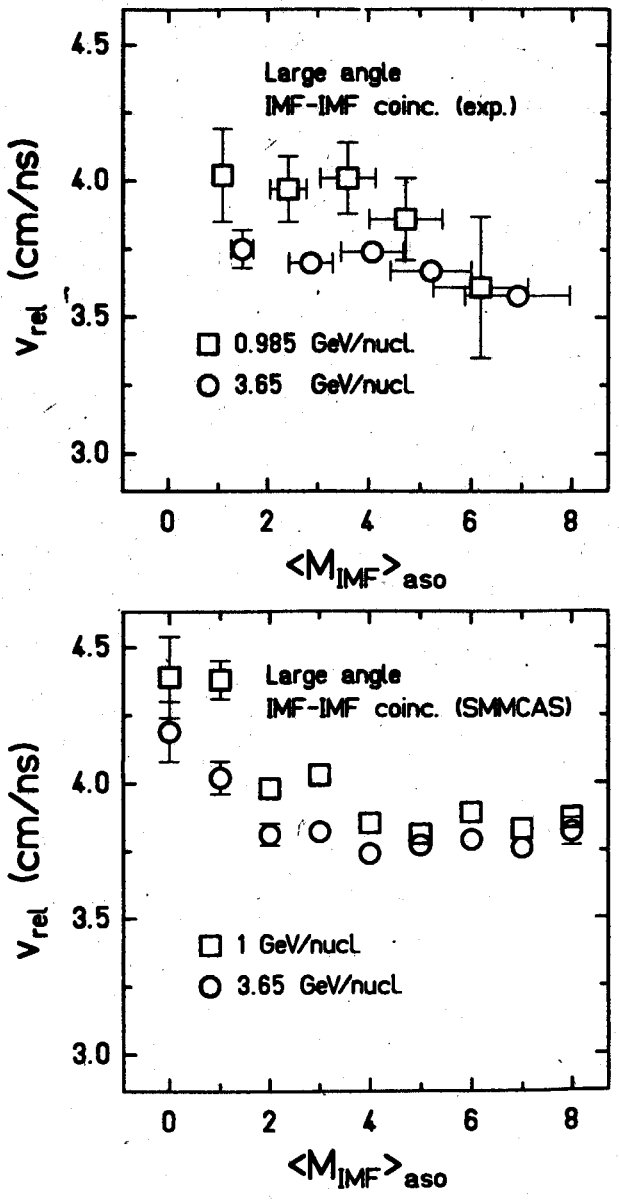

Figure 7: The mean relative velocities at large correlation angles as a functio the associated IMF–multiplicity. Upper part — experimental data for two inci ^4He–energies; bottom part — data, calculated by the cascade–fragmentation mo

the fragment multiplicity. This could be related to a bigger freeze–out volume for the high multiplicity events. A more definite conclusion needs further calculations.

Information on the time scale of the multifragmentation process can be obtained from the study of the angular correlation between coincident fragments at the small correlation angles. When the time interval between the emission of the fragments in the same event is short, the small relative angles are supressed due to Coulomb repulsion of the coincident IMF's. This effect is evident from Fig. 8, which presents the two–fragment correlation functions $R_{12}(\theta_{rel})$, defined as $R_{12} = CY_{1,2}(\theta_{1,2})/Y_{1^*,2}$, where Y_{12} is the yield of coincidences between trigger 1 and fragment 2. The denominator $Y_{1^*,2}$ gives a coincidence rate for the same counter of FMD, but for another trigger 1^* for which $\theta_{1^*,2} > 90°$. This normalization reduces a systematical error due to uncertainties in the detector efficiency. These distributions show a significant depletion of the coincidences at the small relative angles. The Z–dependence of this effect is evident from comparison of the left and right parts of Fig, 8: the supression of the coincidence rate at the small angles becomes stronger, when the product of Z–values of the fragments detected is increased three times. The quantitative analysis of the data is in progress now. It is expected from the magnitude of the effect observed that the mean life–time of the system is not larger than 10^{-21} s.

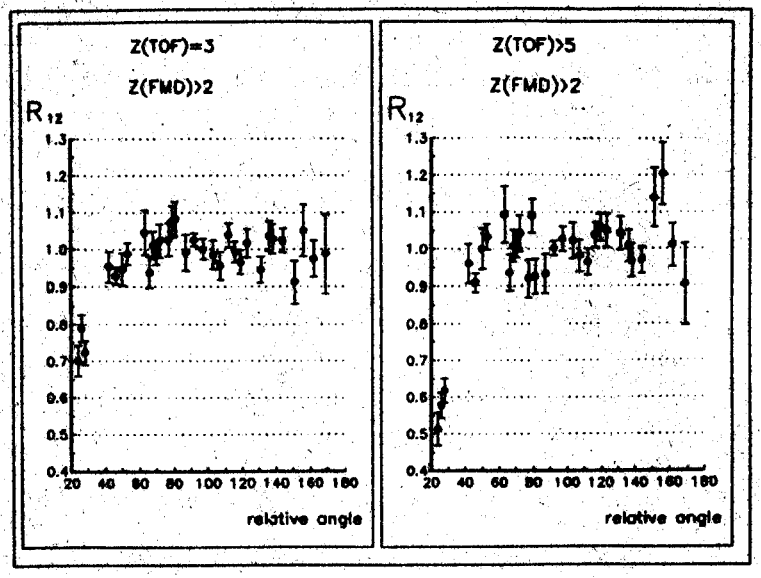

Figure 8: Two fragment correlation function measured for $^4He + Au$ collisions at 3.65 GeV/nucl. The Z–values of the detected fragments are shown in the upper part of the figure.

6 Conclusion

— Multifragment emission is a dominant decay mode of the highly excited target spectator for $^4He + Au$ collisions at the energies (1–4) GeV/nucl.
— The mean multiplicity for an intermediate mass fragments at higher incident energy used is $< M_{IMF} >= 5.3 \pm 0.8$. From the comparison of the experimental data and the statistical model calculation we conclude that the excitation energies reached are higher than 1 GeV.
— The mass spectrum of IMF is fitted well by a power law distribution $A^{-\tau}$. Parameter τ shows "critical behaviour" (a minimum) as a function of LCP–multiplicity (excitation energy), which can be related to the effect of a secondary decay of the excited fragments.
— The breakup density of the system was estimated from the relative velocities of the coincident fragments at large correlation angles. It was found to be at least three times smaller than the normal one.
— The small relative angles between fragments are supressed because of the Coulomb repulsion and a short time scale of the multifragmentation process.
— The use of a light projectile like ^4He at relativistic energies in the multifragmentation study gives complementary information to that obtained from heavy ion collisions. In our case the dynamical effects are reduced and decay of the excited nucleus (target spectator) proceeeds in an apparently statistical manner ("thermal multifragmentation").

This work is supported in part by Russian Fundamental Research Foundation under Project No 93–02–3755 and by Bundesministerium für Forschung und Technology under Contract No 06 DA 453.

We would like to thank Profs. E. Kankeleit, S.T. Belyaev, A.M. Baldin, Ts. Vylov, A.N. Sissakian for their support.

References

[1] L.C. Moretto and G.J.Wozniak, *Progr. Part and Nucl. Phys.* **21** (1988) 460.
[2] W. Friedman, *Phys. Rev. Lett.* **60** (1988) 2125;
Phys. Rev. **C42** (1990) 667.
[3] J. Bondorf, R. Donangelo, I.N. Mishustin, C.J. Pethick, H. Schulz, *Nucl. Phys.* **A443** (1985) 321;
J. Bondorf, R. Donangelo, I.N. Mishustin, H. Schulz, *Nucl. Phys.* **A444** (1985) 460.
[4] D.H.E. Gross, *Nucl. Phys.* **A428** (1985) 313c;
Sa Ban-Hao, D.H.E. Gross, *Nucl. Phys.* **A437** (1985) 643.
[5] P.J. Siemens, *Nature* **305** (1983) 410;
A.D. Panagiotou, M.W. Curtin, D.K. Scott, *Phys. Rev.* **C31** (1985) 55.
[6] L.G. Moretto, Kin Tso, N. Colonna, G.J. Wozniak, *Phys. Rev. Lett.* **69** (1992) 1884.
[7] W. Bauer, G.F. Bertsch, H. Schulz, *Phys. Rev. Lett.* **69** (1992) 1888.
[8] D. Fox, R.T. de Souza, L. Phair, D.R. Bowman, N. Carlin, C.K. Gelbke, W.G. Gong, Y.D. Kim., M.A. Lisa, W.G. Lynch, G.F. Peaslee, M.B. Tsang, F. Zhu, *Phys. Rev.* **C47** (1993) R421.
[9] T. Li, W. Bauer, D. Graig, M. Cronqvist, E.Gualtieri, S. Hannuschke, R. Lacey, W.J. Llope, T. Reposeur, A.M. Vander Moden, G.D. Westfall, W.K. Wilson, J.S. Winfield, J. Lee, S.J. Yennello, A. Nadasen, R.S. Tickle, E. Norbeck, *Phys. Rev. Lett.* **70** (1993) 1924.
[10] B.V. Jacak, *Nucl. Phys.* **A488** (1988) 352c.
[11] J. Hubele, P. Kreutz, V. Lindenstruth, J.C. Adloff, M. Begemann-Blaich, P. Bouissou, G. Imme, I. Iori, G.J. Kunde, S. Leray, Z. Liu, U. Lynen, R.J. Meijer, U. Milkau, A.Moroni, W.F. Müller, C. Ngo, C.A. Ogilvie, J.Pochodzalla, G. Raciti, G.Rudolf, H. Sann, A. Schüttauf, W. Seidel, L. Stuttge, W. Trautmann, A. Tucholski, R. Heck, A.R. De Angelis, W.A. Friedman, H.R. Charity, *Phys. Rev.* **C46** (1992) R1577.
[12] G. Klotz-Engman, H. Oeschler, J. Stroth, E. Kankeleit, Y. Cassagnon, M. Conjeaud, R. Dayras, S. Harar, R. Legrain, E.C. Pollacco, C. Volant, *Nucl. Phys.* **A499** (1989) 392.
[13] R. Trockel, U. Lynen, J. Pochodzalla, W. Trautmann, N. Brummund, E. Eckert, K. Glasow, K.D. Hildenbrand, K.H. Kampert, W.F.J. Müller, D. Pelte, H.J. Rabe, H. Sann, R. Santo, H. Stelzer, R. Wada, *Phys. Rev. Lett.* **59** (1987) 2844.
[14] S.P. Avdeyev, V.A. Karnaukhov, W.D. Kuznetsov, L.A. Petrov, R. Barth, V. Lips, H. Oeschler, O.V. Bochkarev, L.V. Chulkov, E.A. Kuzmin, I.G. Mukha, V.A. Olkin, G.B. Yankov, W. Karcz, Y.T. Vidaj, W. Neubert, E. Norbeck, *Nucl. Instr. and Meth. A* (1993) .
[15] A.S. Botvina, A.S. Iljinov, I.N. Mishustin, *Nucl. Phys.* **A507** (1990) 649; A.S. Botvina, I.N.Mishustin, *Phys. Lett.* **B294** (1992) 23.
[16] J. Hubele, P. Krentz, J.C.Adloff, M. Begemann-Blaich, P. Bouissou, G. Imme, I. Iori, G.J. Kunde, S. Leray, V. Lindenstruth, Z. Liu, U. Lynen, R.J. Meijer, U. Milkau, A. Moroni, W.F.J. Müller, C. Ngo, C.A. Ogilvie, J. Pochodzalla, G. Raciti, G. Rudolf, H. Sann, A. Schüttauf, W. Seidel, L. Stuttge, W. Trautmann, A. Tucholski, *Z. Phys.* **A340** (1991) 263.
[17] D.H.E. Gross, G. Klotz-Engmann, H. Oeschler, *Phys. Lett.* **B224** (1989) 29.
[18] J. Pochodzalla, W. Trautmann, U. Lynen, *Phys. Lett.* **B232** (1989) 41.

Received by Publishing Department on July 20, 1993.